Aspects of Molecular Medicine 2 (2023) 100031

Contents lists available at ScienceDirect

Aspects of Molecular Medicine

journal homepage: www.journals.elsevier.com/aspects-of-molecular-medicine

Mefenamic acid inhibit transforming growth factor-beta type-1: Repurposing anti-inflammatory drugs in wound healing using in-silico approaches

Miah Roney [a,b], Abdul Rashid Issahaku [c,d], Normaiza Binti Zamri [a], Mohd Fadhlizil Fasihi Mohd Aluwi [a,b,*]

[a] Faculty of Industrial Sciences and Technology, Universiti Malaysia Pahang Al-Sultan Abdullah, Lebuhraya Tun Razak, 26300 Gambang, Kuantan, Pahang Darul Makmur, Malaysia
[b] Centre for Bio-Aromatic Research, Universiti Malaysia Pahang Al-Sultan Abdulah, Lebuhraya Tun Razak, 26300 Gambang, Kuantan, Pahang Darul Makmur, Malaysia
[c] Department of Chemistry, University of the Free State, 205 Nelson Mandela Avenue, Bloemfontein 9301, South Africa
[d] West African Centre for Computational Research and Innovation, Ghana

ARTICLE INFO

Handling Editor: Prof A Angelo Azzi

Keywords:
Mefenamic acid
In-silico
Wound healing
Docking
MD simulation

ABSTRACT

Due to low cost and time-saving benefits, drug repurposing is a safe and successful method to discover drug. A druggable target for inflammation, transforming growth factor-beta type-1 (TGF-β 1) has been identified to be associated with wound healing. Finding the most effective TGF-β 1 inhibitor among FDA-approved anti-inflammatory medications was the goal of the current investigation. To find the best hits against TGF-β 1, we used structure-based virtual screening on medications that have received FDA approval. We discovered two FDA-approved medications with notable selectivity and affinity for the binding pocket of TGF-β 1. Mefenamic acid, one of these found hits, interacts with key TGF-β 1 residues and favourably attaches to the binding pocket, requiring further study. The kinetics of the binding between mefenamic acid and TGF-β 1 were revealed by all-atom precise molecular dynamics (MD) simulations. Mefenamic acid, which may also be used as a possible lead chemical against TGF-β 1, may be a promising TGF-β 1 inhibitor.

1. Introduction

The complicated and multifaceted process that occurs in reaction to a disruption of the normal anatomical structure and function of a skin tissue is referred to as wound healing. It is characterised by a number of events, including inflammation, the cellular phase (granulation), the shrinking of the wound area (wound contraction), the synthesis of collagen, the covering of the epithelium (epithelialization), and the remodelling of the scar (cicatrization). All these processes flow together to successfully complete wound healing and restore the skin's disorganised anatomical and functional condition (Ibrahim et al., 2018). The materials employed in the wound dressing can have a significant impact on wound care and the effectiveness of wound healing in occluding the wounded tissue (Hajialyani et al., 2018). It is a worldwide problem to design and produce an adequate wound dressing for the healing of both acute and chronic wounds (Yazarlu et al., 2021). A wealth of knowledge on the function of conventional treatments in addressing the underlying causes of nonhealing wounds is available in several research. Traditional wound healing therapies have been explored experimentally and therapeutically including cell culture-based, animal and human-based studies.

The three different proteins TNF, TGFBR1, and IL-1β play key roles in wound healing (Shady et al., 2022). Among them, a protein called transforming growth factor (TGF) is a transmembrane serine/threonine kinase that phosphorylates SMAD proteins, leading to their dimerization and transport to the nucleus, where gene transcription takes place (Harikrishnan et al., 2018). TGF-β is crucial for the formation of the extracellular matrix (ECM) and for promoting the chemotaxis of fibroblast cells. Granulation tissue forms as a result of the proliferative phase of the fibroblast process, giving the wound a reddish appearance. Three isoforms of TGF-β have been found; transforming growth factor beta 1 (TGF-β receptor type-1) is one of these isoforms can influence

* Corresponding author. Faculty of Industrial Sciences and Technology, Universiti Malaysia Pahang Al-Sultan Abdullah, Lebuhraya Tun Razak, 26300 Gambang, Kuantan, Pahang Darul Makmur, Malaysia.
E-mail address: fasihi@umpsa.edu.my (M.F.F. Mohd Aluwi).

https://doi.org/10.1016/j.amolm.2023.100031
Received 13 August 2023; Received in revised form 5 November 2023; Accepted 19 November 2023
Available online 25 November 2023

mesenchymal cell differentiation and proliferation as well as boost the synthesis of extracellular matrix (ECM) during wound healing (Aida et al., 2022). Additionally, the target is TGF-β receptor type-1, which plays a crucial role in wound healing through regulation of the process of cell differentiation and proliferation rather than its modulatory effect on the immune response (Shady et al., 2022).

It takes time and money to produce a new medication; development timeframes sometimes exceed 10 years, and costs can range from $800 million to $1.2 billion (Hamed et al., 2014). A more recent method for creating secure and efficient medicines against illnesses is drug repurposing (Atiya et al., 2023). While virtual screening, which has demonstrated considerable potential in the field of drug development, will be crucial in locating lead (active) compounds in databases (Shen et al., 2003). The creation of tiny molecules that act as disease inhibitors has been ongoing over the past five years. This effort includes high throughput screening, testing of natural compounds, rational drug design synthesis, and virtual screening utilising computer-aided drug design (CADD) (Dighe et al., 2019). Additionally, drug repurposing offers a number of advantages with little financial outlay and high returns. The new medicine candidate has a decreased probability of failure because it has previously successfully completed many studies. The main benefit of medication repurposing is that it makes use of the various action routes and targets that a medicine can use. Because the information on medication toxicity is already available and processing time is drastically cut, safety is another benefit of drug repurposing (Atiya et al., 2023).

Here, we used structure-based virtual screening to discover possible TGF-β 1 kinase domain inhibitors from the FDA-approved anti-inflammatory drugs (Table S1). In order to locate FDA-approved anti-inflammatory medications, we examined the literature library. Then, we virtually screened these medications against TGF-β 1 kinase domain receptor, which is a potent druggable target for wound healing. The top hit compound out of the top two compounds (Ketorolac and Mefenamic acid) that we found was chosen for more in-depth research. Pharmacological characteristics were used to interpret the druggability score of the lead compound (Mefenamic acid). Furthermore, to understand the binding and conformational dynamics of the TGF-β 1-Mefenamic acid complex, a thorough investigation utilising molecular dynamics (MD) simulation research was performed on the leading medication.

2. Methodology

2.1. Virtual screening

Using the protein-ligand docking approach, we generated a library of 20 FDA-approved anti-inflammatory medicines (Table S1) and conducted virtual screening for the target transforming growth factor-beta type-1 (TGF-β 1). The Protein Data Bank's PDB ID 6B8Y was used to locate the crystal structure of TGF-β 1. The online docking programme Cavity-detection guided Blind Docking (CB-Dock) was used to estimate the docking analysis using the virtual screening techniques mentioned before (Roney et al., 2023a,b,c). Molecular docking-based virtual screening in a blind search space was carried out using the CB-Dock programme. The structures of co-crystallized ligand and FDA-approved anti-inflammatory medicines were built using ChemSketch programme. To see the bond conformations and binding affinities of ligands with TGF-β 1, docking analysis was used. When the virtual screening was finished using CB-Dock, the screening findings were examined, and the best docked conformations were then taken for additional examination.

2.2. Re-docking

Using the Discovery Studio 3.1 (DS3.1) software and the Rullah et al. method, the elucidated drugs from the virtual screening study and the co-crystal were taken for re-docking analysis with TGF-β 1 (Rullah et al., 2023). The co-crystal was re-docked into the designated binding site in order to replicate the co-crystal's binding posture as the original ligand in 6B8Y, therefore validating the docking process. Among the top-ranking conformation clusters from the dock, the difference between the redocked and original posture was evaluated using the root-mean-square deviation (RMSD) value. For the docking approach, the process that resulted in a docked result with a low RMSD value (below 2.0 Å) was used.

2.3. Pharmacological properties

To test the theoretical pharmacokinetics and forecast the drug-likeness of the ligands, mefenamic acid and co-crystal were assessed using ADMET restrictions in accordance with Lipinski's rule of five and oral bioavailability. Effective drug-like molecules are those compounds that adhere to three or more of the five criteria. Molecular descriptors for Lipinski's rule were examined using the online prediction tool Molsoft L.L.C. (Molecular characteristics and drug likeliness) (Panchal et al., 2021). A drug-likeliness score (between −1 and +1) is provided by the programme along with scores for each of the five categories.

2.4. Molecular dynamic (MD) simulation

Beginning with the lead protein-Mefenamic acid and protein-reference chemical complexes chosen from the molecular docking, all atom-based molecular dynamics simulations were performed. Using the AMBER20 programme, the MD simulations were carried out (Roney et al., 2023a,b,c). The system was separated by 10 Å before the addition of a truncated octahedral TIP3P water box. Additionally, hydrogen atoms were added to the system using the LEaP module, and the charge in the system was subsequently neutralised with Na^+/Cl^- ions. The NVT system simulation was ran for 500 ps at the maintenance temperature of 310.15 K in order to additionally distribute the solvent molecules equally throughout the water box. Finally, simulations of two complexes—Protein-Mefenamic acid and Protein-reference compound—were employed for a 100 ns NPT system with periodic threshold requirements.

2.5. Free energy calculations of TGF-β 1-mefenamic acid and reference compound complexes

The binding free energy between the protein and ligand for each system was calculated using the MM-GBSA method (Roney et al., 2023a,b,c). This study's estimate used a 100 ns MD trajectory. The calculation equations are as follows:

$$\Delta G_{bind} = E_{gas} + G_{sol} - TDS$$

$$E_{gas} = E_{int} + E_{vdw} + E_{ele}$$

$$G_{sol} = G_{GB} + G_{non\text{-}polar}$$

$$G_{non\text{-}polar} = \gamma SASA + b$$

E_{gas} is the total of the internal energy terms for the AMBER force field, where ΔG_{bind} is assumed to be the sum of the gas phase and solvation energy terms less the entropy (TDS) term. Covalent van der Waals (E_{vdw}), E_{int} (bond, angle, and torsion), and the non-bonded electrostatic energy component (E_{ele}).

3. Results and discussion

3.1. Docking-based virtual screening

The drug development process benefits greatly from computational techniques (Atiya et al., 2023). In-silico virtual screening describes macromolecule-ligand interactions using computer models (Murgueitio

et al., 2012). We virtually screened the 20 medications to identify the high-affinity TGF-β 1 binding partners (Table S2). We discovered that several of the medicines that were screened exhibit a significant binding affinity score towards the TGF-β 1 binding pocket and may thus be further chosen for in-depth study. Out of 20 medicines with significant binding affinities to TGF-β 1 that were found by screening of the output, two were found to be hits (Table 1). With the co-crystallized ligand (PDB ID: 6B8Y), both medications exhibit equal affinity towards TGF-β 1.

The DS3.1 was then used to re-dock the chosen two medicines, and interacting residue interactions were used to analyse binding modes and interaction patterns (Table 2). Before re-docking procedure, we validated the software by docking the co-crystal in the docking site of 6B8Y protein and compared the RMSD value with the original pose of co-crystal. The docked co-crystal conformation that was recovered is superposed over the co-crystallized ligand in Fig. 1. The docking algorithm utilised is effective in predicting the binding mode of the ligands, as evidenced by the 0.11 Å RMSD value between the redocking co-crystal and binding posture crystallized co-crystal, which was less than 2.0 Å.

Based on the molecular docking study, the selected two compounds (ketorolac and mefenamic acid) bound in the active site of target protein with the binding energy of −39.1791 and −41.5397 kcal/mol, respectively. Important TGF-β 1 residues, such as Val219, Ala230, Lys232, Leu260, and Leu340, were shown to interact with two medications, ketorolac and mefenamic acid, in a substantial number of ways (Figs. 2 and 3). These findings, which were thoroughly examined, indicate that ketorolac and mefenamic acid have distinct interactions with the bonding pocket of TGF-β 1. Ketorolac is stabilised by multiple alkyl and pi-alkyl bonds with the residues Ala230, Leu260, Val219, Leu340, and Ile211, as well as a tight hydrogen link with His283 (2.43 Å) (Fig. 2A and B). Similar to this, mefenamic acid makes a number of alkyl and pi-alkyl connections with the residues of Val219, Leu260, Lys232, Ala230, and Leu340 (Fig. 3A–B), as well as two hydrogen bonds with Tyr249 (1.86 Å) and Asp351 (2.30 Å).

Additionally, four hydrogen bonds with the residues His283 (2.62 Å), Tyr249 (4.11 Å), Lys232 (4.43 Å), and Asp351 (2.11 Å), as well as a number of alkyl and pi-alkyl bonds with the residues of Ile211, Leu340, Ala350, Val219, Leu278, Ala230, and Tyr249, all contribute to the co-crystal's stabilisation. Additionally, the Asn338, Lys332, Lys337, Asp281 and His283 residues of the co-crystal displayed hydrophobic interactions with one another (Fig. 4A–B).

TGF-β 1 was used to investigate the pharmaceutical medicines ketorolac and mefenamic acid for their intricate interactions. The interactions graphs demonstrated that ketorolac binds to His283 in a hydrogen bond in addition to other interactions. Mefenamic acid also engages in a number of hydrophobic interactions and creates hydrogen bonds with Tyr249 and Asp351. Both medications have a number of

Table 1
List of selected drugs based on the binding affinity and H-Bs with TGF-β 1 using the CB-Dock for virtual screening purpose.

Compound Name	Vina Score	No. Of H–B	Bound Amino acids
Ketorolac	−9.0	9	Ala264, Leu278, Val231, Ala230, Val 279, Tyr249, Gly 261, Asp281, Gly286 (H–B), Glu245, Leu278, Lys232, Val219, Tyr249, Ile211, Ala230, Leu260, Leu340 (*C*–H), Lys232, His283 (ionic)
Mefenamic acid	−9.2	7	Leu278, Val231, Ala230, Trp 220, Asp281, Tyr249, Gly286 (H–B), Glu245, Val219, Tyr249, Leu260, Ile211, Ala230, Leu340 (*C*–H), Lys232 (pi-cation), Lys232, His283 (ionic)
Co-Crystal	−11.6	10	Gly286, Tyr249, Asn338, His283, Val231, Leu278, Ala230, Ser 280, Asp281, Ala264 (H–B), Leu260, Asn338, Leu340, Ala230, Ile211, Val219, Lys232, Leu278, Glu245, Phe 262, Tyr249 (*C*–H), Lys232, His283 (ionic)

Table 2
Re-docking interaction energy to select the lead drug against TGF-β 1 using the DS3.1

Compound Name	CDOCKER Interaction Energy	Bound Amino Acids
Ketorolac	−39.1791	His283 (2.43) (H–B), Lys232 (pi-cation), Ala230, Leu260, Val219, Leu340, Ile211 (alkyl/pi-alkyl)
Mefenamic acid	−41.5397	Tyr249 (1.86), Asp351 (2.30) (H–B), Val219, Leu260, Lys232, Ala230, Leu340 (alkyl/pi-alkyl)
Co-crystal	−53.445	His283 (2.62), Tyr249 (4.11), Lys232 (4.43), Asp351 (2.11) (H–B), Asn338, Lys332, Lys337, Asp281, His283 (*C*–H), Glu245 (halogen), Ile211, Leu340, Ala350, Val219, Leu278, Ala230, Tyr249 (alkyl/pi-alkyl)

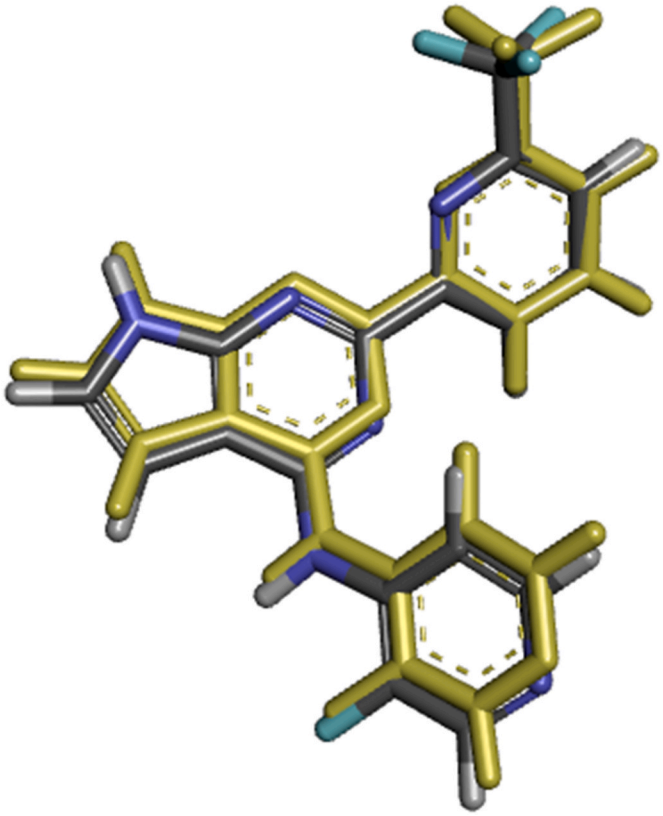

Fig. 1. Overlaying the co-crystal recovered from the protein crystal structure with the redocked conformation of the co-crystal. The redocked co-crystal is shown in yellow, while the original co-crystal is shown in black. (For interpretation of the references to colour in this figure legend, the reader is referred to the Web version of this article.)

TGF-β 1 interactions in common. A number of well-known small molecules including TGF-β 1 revealed structural similarities with ketorolac and mefenamic acid. Mefenamic Acid demonstrated particular and noteworthy binding energy and interactions with TGF-β 1 protein, according to the findings and discussion. These results suggest that mefenamic acid may be used as wound healing agent. The starting point for our stability MD simulations was the chosen posture for mefenamic acid.

3.2. *Pharmacological property*

The findings suggest that mefenamic acid adhered to four of

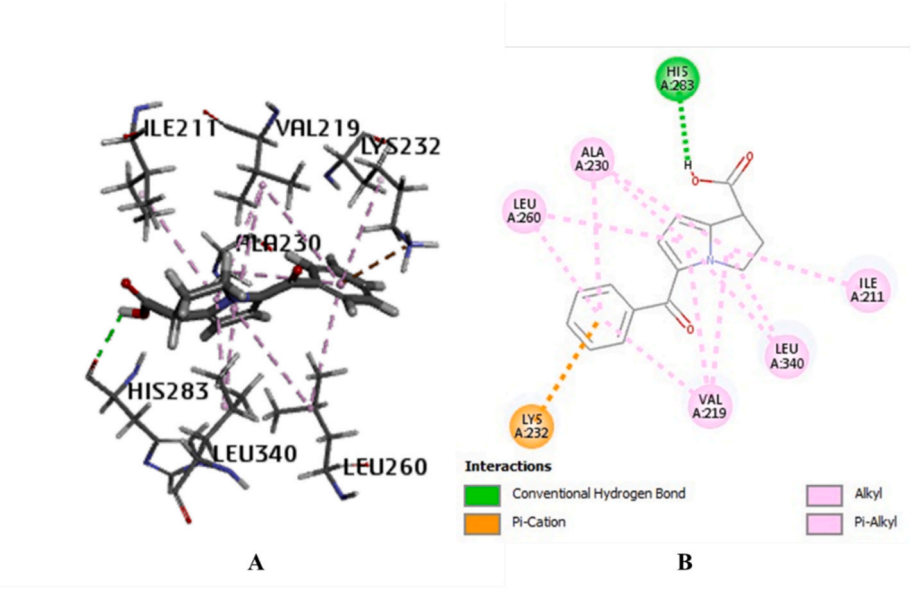

Fig. 2. TGF-β 1 interactions with Ketorolac. (A) 3D view of TGF-β 1 with Ketorolac. (B) 2D view of TGF-β 1 with Ketorolac.

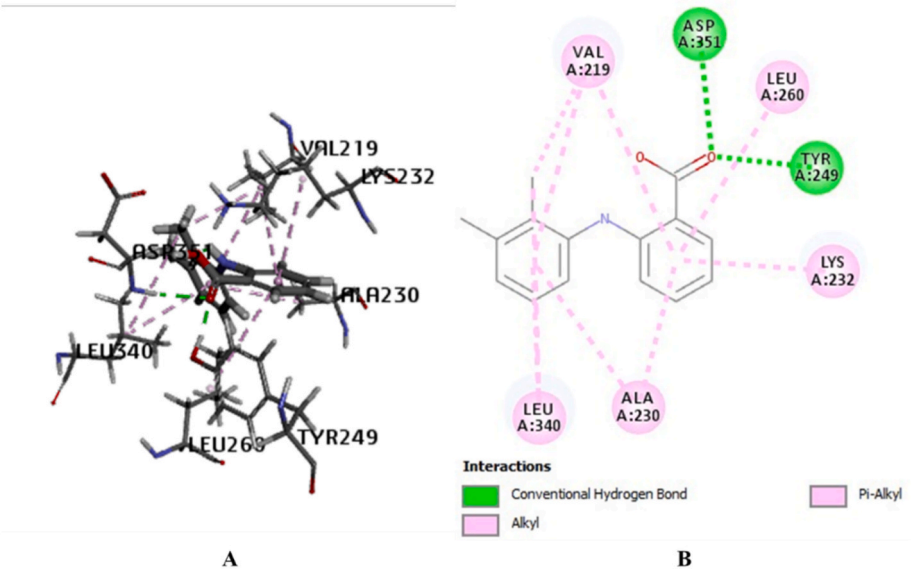

Fig. 3. TGF-β 1 interactions with Mefenamic acid. (A) 3D view of TGF-β 1 with Mefenamic acid. (B) 2D view of TGF-β 1 with Mefenamic acid.

Lipinski's rules: the molecular weight had to be below 500 Da, the H-bond acceptor had to be below 5, the H-bond donor had to be below 10, and the refractive molar range had to be between 40 and 130 cm^3. The co-crystal adhered to all of Lipinski's criteria (Table 3). Mefenamic acid did not exhibit the anticipated value as the co-crystal, but it still passed Lipinski's tests with a predicted drug-likeliness model score of 0.29 (Fig. 5a), which is at the high end of the scale for a compound's drug-likeliness, and a predicted drug-likeliness model score of 0.36 (Fig. 5b), which is at the predicted value for the co-crystal. As a result, it may be said that mefenamic acid also shown a higher likelihood of success for drug-likeness research.

3.3. Molecular dynamic (MD) simulation

The protein backbone RMSD calculated from the MD simulation trajectory was used to assess the stability of protein-Mefenamic acid and protein-reference chemical complexes. Proteins are more likely to be folded when the RMSD is lower and more likely to be unfolded when the RMSD is higher (Costa et al., 2022). Low fluctuation or continuous variance in RMSD are indicators of system equilibration. Fig. 6 displays the estimated RMSD of the TGF-β receptor type-1 backbone for each frame. The protein backbone RMSD gradually increased up to around 20 ns, as seen in Fig. 6, and then it stabilised until the simulation was over. No uncommon or abnormal backbone deviations were found. When doing an MD simulation, the protein deviation may be estimated using the average RMSD of the backbone. The backbone of the TGF-β receptor type-1 was found to have an average RMSD of 1.86 ± 0.28 Å.

It's critical to monitor the ligand's departure from its native structure during the MD simulation. The outcome of the ligand-RMSD calculation is displayed in Fig. 7. The simulation revealed that mefenamic acid and the reference compounds remained essentially unchanged. As shown in Table 4, the mefenamic acid and reference compound RMSDs were calculated to be 1.91 ± 0.35 Å and 1.64 ± 0.30 Å, respectively. Furthermore, the low RMSD and continuous fluctuation show that the

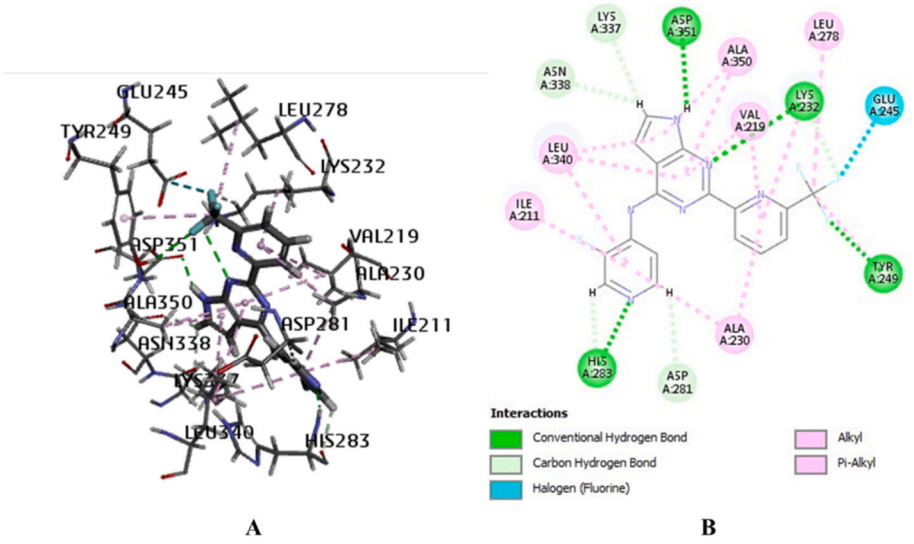

Fig. 4. TGF-β 1 interactions with Co-crystal. (A) 3D view of TGF-β 1 with Co-crystal. (B) 2D view of TGF-β 1 with Co-crystal.

Table 3
Pharmacological properties for Mefenamic acid and co-crystal predicted by Lipinski's rule of five for oral bioavailability using Molsoft L.L.C. software.

Parameter		Mefenamic acid		Co-crystal	
	Acceptance criteria	Score	Complies/does not comply	Score	Complies/does not comply
Molecular weight	<500 Da	241.11	Complies	374.09	Complies
H-bond acceptor	<5	2	Complies	4	Complies
H-bond donor	<10	2	Complies	2	Complies
Mol LogP	<5	5.10	Does not comply	3.79	complies
Molar refractivity	40–130 cm^3	72.88 cm^3	Complies	89.42 cm^3	Complies
Drug-likeness score	–	0.29	0.29	0.36	0.36

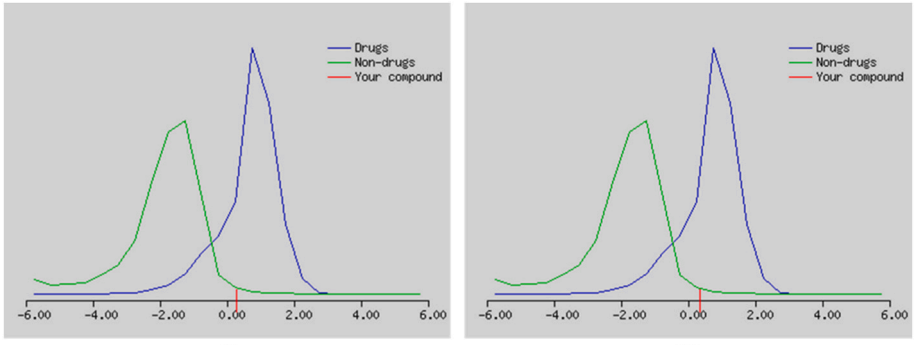

Fig. 5. The Drug-likeliness model score for (a) Mefenamic acid (b) co-crystal were predicted using Molsoft L.L.C. software to be 0.29, indicating that Mefenamic acid possesses drug-like properties for oral formulation based on bioavailability.

protein-ligand combination was stable throughout the experiment (Hasan et al., 2022).

In order to achieve the stability of the complex with the ligand, the amino acid residues of the protein play a crucial role (Patel et al., 2021). The variability of certain amino acid residues may be studied using the RMSF parameter. Fig. 8 displays the outcomes of calculating the RMSF for each amino acid in the TGF-β receptor type-1 using MD simulation trajectories. It was discovered that the TGF-β receptor type-1 amino acids varied similarly when bound to mefenamic acid and the reference substance. The distinction between the maximum and average RMSF might shed light on the variability of the simulation. The values were determined to be 10.89 ± 3.47 Å and 12.63 ± 0.4.16 Å with Mefenamic acid and reference drug, respectively, when the RMSF of TGF-β receptor type-1 Apo protein was 7.02 ± 2.24 Å. However, these significant oscillations were shown to be caused by loop sections extending in protein structural conformations, which are located outside of the binding pocket.

The RoG, computed from the MD simulation trajectory, was utilised to look into the compactness of the Mefenamic acid and reference compound-bound TGF-β receptor type-1. Fig. 9 displays the computed RoG for each system. It's interesting to see that the system stayed small throughout the test. The difference in RoG values between the highest and lowest TGF-β receptor type-1 Apo protein was calculated to be 0.71 Å; the values for the proteins bound to Mefenamic acid and the reference compound were 0.86 Å and 0.70 Å, respectively. Compactness and little deviation provided an explanation for the complexes' rigidity and stability.

Protein interactions with the ligand were shown throughout through

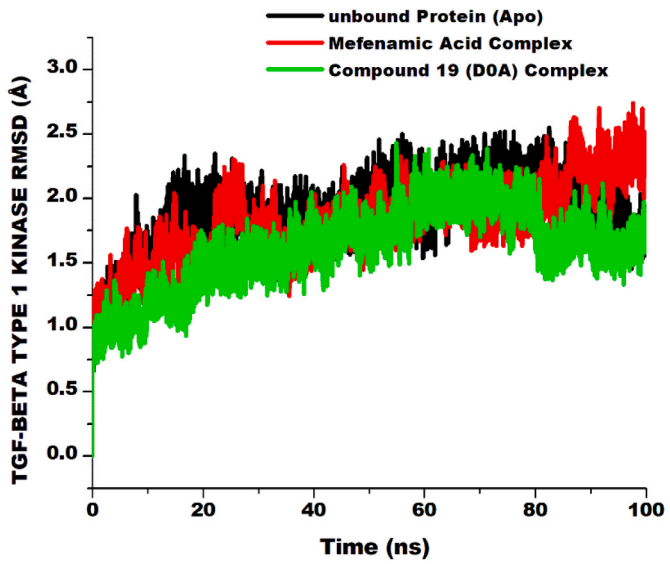

Fig. 6. RMSD plot of 100 ns MD simulation of TGF-β 1 in (black) apo and complex with (red) Mefenamic acid and (green) co-crystal. (For interpretation of the references to colour in this figure legend, the reader is referred to the Web version of this article.)

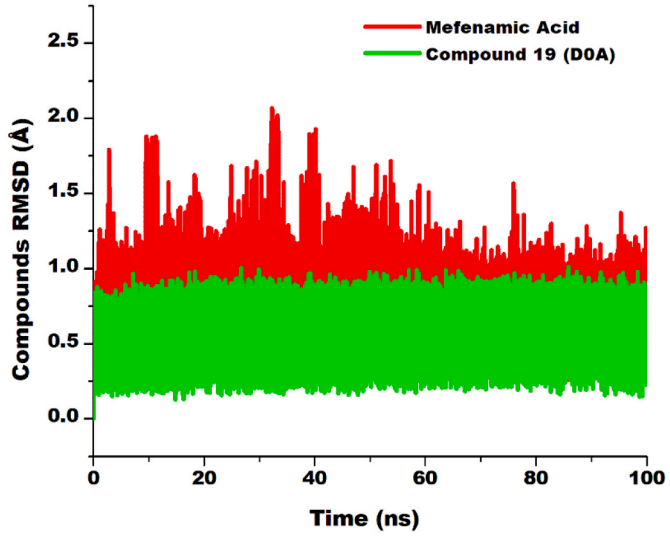

Fig. 7. RMSD plot of 100 ns MD simulation of (red) Mefenamic acid and (green) co-crystal. (For interpretation of the references to colour in this figure legend, the reader is referred to the Web version of this article.)

the simulation (Fig. 10). H-bond interaction study is necessary to comprehend the stability of the proposed protein-ligand combination. H-bonding facilitates the ligand's capacity to enter the binding site. Hydrogen bonding (H–B) is one of the most powerful non-covalent binding interactions; a higher value indicates greater binding. According to the experimental results, the simulation's latter stages were essentially when the hydrogen bond counts of two complexes were at their peak. The protein-Mefenamic acid and protein-reference compound hydrogen bonding diagrams of the complex were not sparser in the latter phases of simulation, indicating that van der Waals and pi-alkyl bonding was the main contributor to their stability. Nevertheless, mefenamic acid created hydrogen connections with Ala230 residues that were discovered during the docking experiment. Furthermore, Lys232, Tyr249, and His283 residues that were also discovered in the docking tests established hydrogen bonds with the reference molecule.

Fig. 11 displays the calculated and tracked SASA of Mefenamic acid and the reference molecule coupled to TGF-β receptor type-1 during simulations. Variations in the solvent accessibility of proteins were accounted for using this parameter. The SASA did not reveal any appreciable variation. As indicated in Table 4, the difference between

Table 5
Free binding energy calculation for protein-Mefenamic acid and protein-reference compound complexes.

System	Energy components (kcal/mol)				
	ΔE_{vdw}	ΔE_{ele}	ΔG_{gas}	ΔG_{sol}	ΔG_{bind}
Mefenamic Acid	−35.70 ± 4.45	−10.49 ± 3.53	−46.19 ± 5.34	16.48 ± 2.61	−29.71 ± 3.99
Compound 19 (D0A)	−53.67 ± 2.74	−29.94 ± 4.36	−83.61 ± 4.89	32.55 ± 2.95	−51.05 ± 3.51

ΔE_{ele} = electrostatic energy; ΔE_{vdW} = van der Waals energy; ΔG_{bind} = total binding free energy; ΔG_{sol} = solvation free energy ΔG = gas phase free energy.

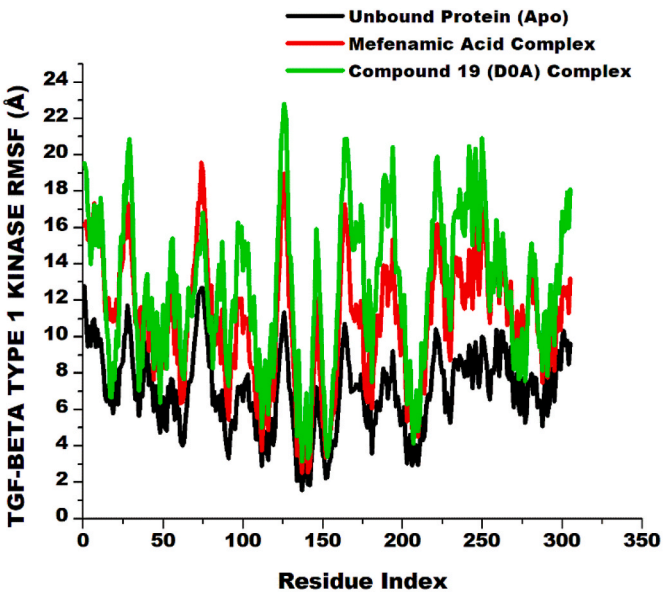

Fig. 8. RMSF plot of 100 ns MD simulation of TGF-β 1 in (black) apo and complex with (red) Mefenamic acid and (green) co-crystal. (For interpretation of the references to colour in this figure legend, the reader is referred to the Web version of this article.)

Table 4
RMSD, RMSF, Radius of Gyration, Hydrogen bonds and SASA analysis for protein-Mefenamic acid and protein-reference compound complexes.

System	Ligand RMSD	RMSD (Å)	RMSF (Å)	RoG (Å)	HB	SASA (A^2)
Apo (Unbound)		1.86 ± 0.28	7.02 ± 2.24	19.75 ± 0.09	159.75 ± 8.12	14,489.65 ± 272.88
Min - Max		0–2.55	1.56–12.75	19.43–20.14	126–193	13,376.54–15,617.66
Mefenamic Acid complex	0.90 ± 0.30	1.91 ± 0.35	10.89 ± 3.47	19.78 ± 0.10	161.52 ± 8.08	14,438.47 ± 332.27
Min - Max	0–2.35	0.00–2.95	2.52–19.55	19.43–20.29	126–202	13,228.65–15,689.81
Reference compound complex	0.60 ± 0.16	1.64 ± 0.30	12.63 ± 0.4.16	19.67 ± 0.09	166.15 ± 8.11	13,835.46 ± 275.95
Min - Max	0–1.01	0–2.43	3.16–22.79	19.35–20.05	133–201	12,706.50–14,966.00

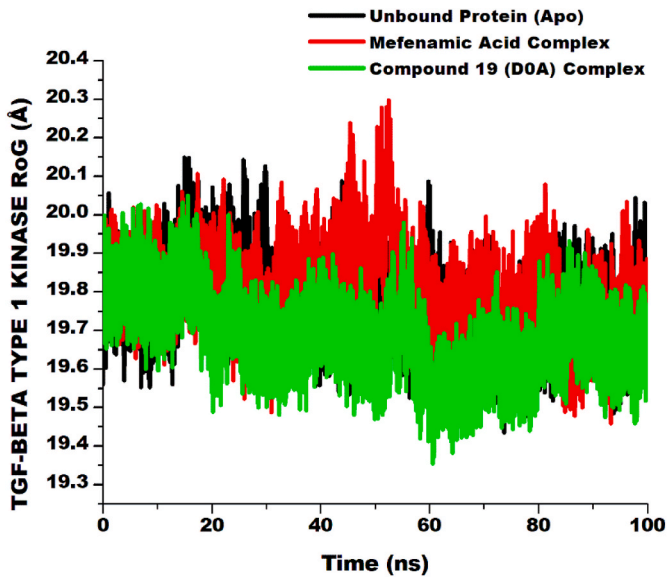

Fig. 9. Radius of gyration plot of 100 ns MD simulation of TGF-β 1 in (black) apo and complex with (red) Mefenamic acid and (green) co-crystal. (For interpretation of the references to colour in this figure legend, the reader is referred to the Web version of this article.)

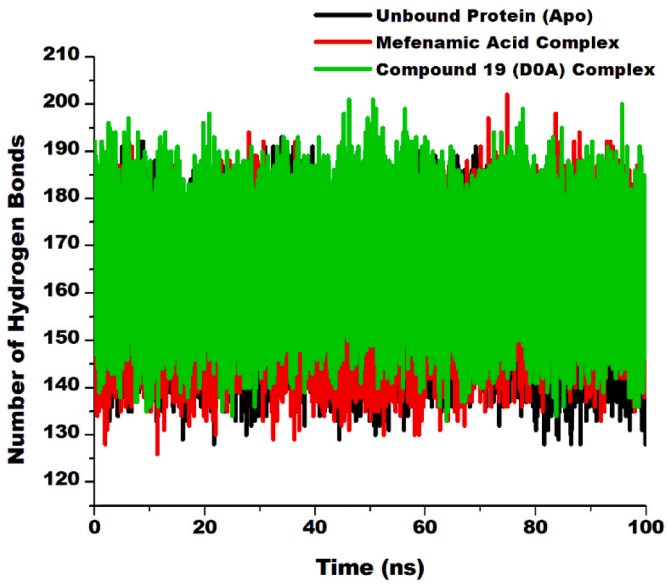

Fig. 10. Hydrogen bonds plot of 100 ns MD simulation of TGF-β 1 in (black) apo and complex with (red) Mefenamic acid and (green) co-crystal. (For interpretation of the references to colour in this figure legend, the reader is referred to the Web version of this article.)

the highest and average SASA for the TGF-β receptor type-1 Apo protein was 1028.01 ± 272.882 $Å^2$, and it was also 1251.34 ± 332.272 $Å^2$ when it was coupled with mefenamic acid and 1130.54 ± 275.952 $Å^2$ when it was coupled with the reference molecule. The overall conclusions from the parameters gained using the MD simulation trajectory have thus clearly defined the stability of the complexes of TGF-β receptor type-1 with Mefenamic acid and the reference molecule.

3.4. Free energy calculations of TGF-β 1-mefenamic acid and reference compound complexes

Based on the trajectory of molecular dynamics simulations, the

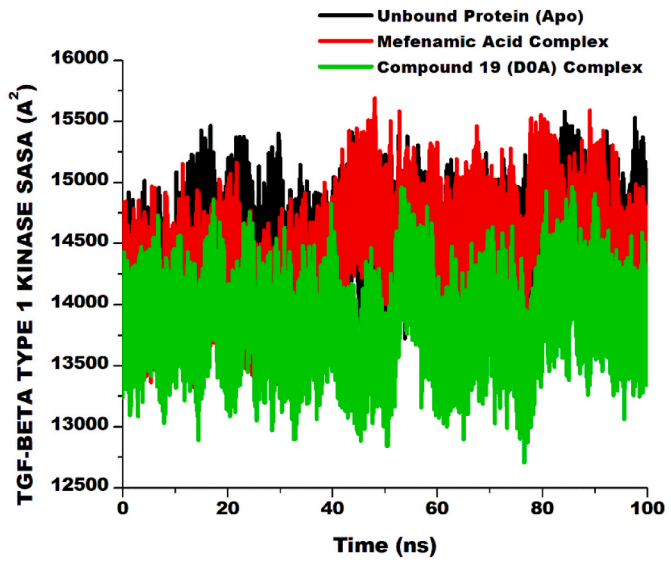

Fig. 11. SASA plot of 100 ns MD simulation of TGF-β 1 in (black) apo and complex with (red) Mefenamic acid and (green) co-crystal. (For interpretation of the references to colour in this figure legend, the reader is referred to the Web version of this article.)

binding free energy was calculated in this work using the MM-GBSA method (Roney et al., 2023a,b,c). The binding free energy can more accurately reflect how tiny compounds and target proteins bind (Wang et al., 2015). The experimental results show that the binding free energies for protein-Mefenamic Acid and protein-reference molecule are, respectively, −29.71 ± 3.99 kcal/mol and −51.05 ± 3.51 kcal/mol (Table 5). Negative values indicate that these two chemicals have a binding affinity to the target proteins, while lower values indicate stronger binding. These chemicals have extraordinarily high binding affinities, according to the simulation results. Most of the binding free energy of these complexes were accounted for by van der Waals and Pi-alkyl interactions.

4. Conclusion

Repurposing licenced medications offers an alternate method for creating secure and efficient therapies for illnesses that are emerging quickly. Here, we used a structure-based, rational, virtual screening method to look for possible TGF-β 1 inhibitors. Following structural and pharmacological investigations, the virtual screening recommended mefenamic acid as a potential TGF-β 1 inhibitor. When it comes to the binding pocket of TGF-β 1 and its essential active residues, this medication exhibits both a notable affinity and specificity. Further analysis of the TGF-b 1-Mefenamic acid complex through all-atom MD simulations for 100 ns on TGF-β 1 and its ligand-bound complexes indicates that TGF-b 1-Mefenamic acid complex will remain stable throughout the simulation trajectory. Moreover, *in-vitro* and *in-vivo* experiments will be used in a wet lab to confirm the current computational findings.

Funding information

No.

Declaration of competing interest

The authors declare that they have no known competing financial interests or personal relationships that could have appeared to influence the work reported in this paper.

Acknowledgments

The authors would like to thank the online software teams.

Appendix A. Supplementary data

Supplementary data to this article can be found online at https://doi.org/10.1016/j.amolm.2023.100031.

References

Aida, A.N., Zhafirah, R., Hirawan, H., Widodo, A.H.B., Prihastuti, C.C., Wardana, T., 2022. Wound healing potential of forest honey for increasing TGF-β1 protein expression in palatoplasty: in-vivo: and: in-silico: studies. Scientific Dental Journal 6 (1), 25–31.

Atiya, A., Das Gupta, D., Alsayari, A., Alrouji, M., Alotaibi, A., Sharaf, S.E., Shamsi, A., 2023. Linagliptin and empagliflozin inhibit microtubule affinity regulatory kinase 4: repurposing anti-diabetic drugs in neurodegenerative disorders using in silico and in vitro approaches. ACS Omega 8 (7), 6423–6430.

Costa, R.A.D., Rocha, J.A.D., Pinheiro, A.S., Costa, A.D.S.D., Rocha, E.C.D., Silva, R.C., Brasil, D.D.S., 2022. A computational approach applied to the study of potential allosteric inhibitors protease NS2B/NS3 from Dengue virus. Molecules 27 (13), 4118.

Dighe, S.N., Dua, K., Chellappan, D.K., Katavic, P.L., Collet, T.A., 2019. Recent update on anti-dengue drug discovery. Eur. J. Med. Chem. 176, 431–455.

Hajialyani, M., Tewari, D., Sobarzo-Sánchez, E., Nabavi, S.M., Farzaei, M.H., Abdollahi, M., 2018. Natural product-based nanomedicines for wound healing purposes: therapeutic targets and drug delivery systems. Int. J. Nanomed. 5023–5043.

Hamed, S., Bennett, C.L., Demiot, C., Ullmann, Y., Teot, L., Desmoulière, A., 2014. Erythropoietin, a novel repurposed drug: an innovative treatment for wound healing in patients with diabetes mellitus. Wound Repair Regen. 22 (1), 23–33.

Harikrishnan, L.S., Warrier, J., Tebben, A.J., Tonukunuru, G., Madduri, S.R., Baligar, V., Borzilleri, R.M., 2018. Heterobicyclic inhibitors of transforming growth factor beta receptor I (TGFβRI). Bioorg. Med. Chem. 26 (5), 1026–1034.

Hasan, A.H., Hussen, N.H., Shakya, S., Jamalis, J., Pratama, M.R.F., Chander, S., Murugesan, S., 2022. In silico discovery of multi-targeting inhibitors for the COVID-19 treatment by molecular docking, molecular dynamics simulation studies, and ADMET predictions. Struct. Chem. 33 (5), 1645–1665.

Ibrahim, N.I., Wong, S.K., Mohamed, I.N., Mohamed, N., Chin, K.Y., Ima-Nirwana, S., Shuid, A.N., 2018. Wound healing properties of selected natural products. Int. J. Environ. Res. Publ. Health 15 (11), 2360.

Murgueitio, M.S., Bermudez, M., Mortier, J., Wolber, G., 2012. In silico virtual screening approaches for anti-viral drug discovery. Drug Discov. Today Technol. 9 (3), e219–e225.

Panchal, R., Bapat, S., Mukherjee, S., Chowdhary, A., 2021. In silico binding analysis of lutein and rosmarinic acid against envelope domain III protein of dengue virus. Indian J. Pharmacol. 53 (6), 471.

Patel, C.N., Jani, S.P., Jaiswal, D.G., Kumar, S.P., Mangukia, N., Parmar, R.M., Pandya, H.A., 2021. Identification of antiviral phytochemicals as a potential SARS-CoV-2 main protease (Mpro) inhibitor using docking and molecular dynamics simulations. Sci. Rep. 11 (1), 20295.

Roney, M., Huq, A.M., Issahaku, A.R., Soliman, M.E., Hossain, M.S., Mustafa, A.H., Tajuddin, S.N., 2023a. Pharmacophore-based virtual screening and in-silico study of natural products as potential DENV-2 RdRp inhibitors. J. Biomol. Struct. Dyn. 1–18.

Roney, M., Issahaku, A.R., Forid, M.S., Huq, A.M., Soliman, M.E., Mohd Aluwi, M.F.F., Tajuddin, S.N., 2023b. In silico evaluation of usnic acid derivatives to discover potential antibacterial drugs against DNA gyrase B and DNA topoisomerase IV. J. Biomol. Struct. Dyn. 1–10.

Roney, M., Singh, G., Huq, A.M., Forid, M.S., Ishak, W.M.B.W., Rullah, K., Tajuddin, S.N., 2023c. Identification of pyrazole derivatives of usnic acid as novel inhibitor of SARS-CoV-2 main protease through virtual screening approaches. Mol. Biotechnol. 1–11.

Rullah, K., Roney, M., Ibrahim, Z., Shamsudin, N.F., Islami, D., Ahmed, Q.U., Mohd Aluwi, M.F.F., 2023. Identification of novel 5-lipoxygenase-activating protein (FLAP) inhibitors by an integrated method of pharmacophore virtual screening, docking, QSAR and ADMET analyses. J. Computat. Biophys. Chem. 22 (1), 77–97.

Shady, N.H., Mostafa, N.M., Fayez, S., Abdel-Rahman, I.M., Maher, S.A., Zayed, A., Abdelmohsen, U.R., 2022. Mechanistic wound healing and antioxidant potential of Moringa oleifera seeds extract supported by metabolic profiling, in silico network design, molecular docking, and in vivo studies. Antioxidants 11 (9), 1743.

Shen, J., Xu, X., Cheng, F., Liu, H., Luo, X., Shen, J., Jiang, H., 2003. Virtual screening on natural products for discovering active compounds and target information. Curr. Med. Chem. 10 (21), 2327–2342.

Wang, L., Wu, Y., Deng, Y., Kim, B., Pierce, L., Krilov, G., Abel, R., 2015. Accurate and reliable prediction of relative ligand binding potency in prospective drug discovery by way of a modern free-energy calculation protocol and force field. J. Am. Chem. Soc. 137 (7), 2695–2703.

Yazarlu, O., Iranshahi, M., Kashani, H.R.K., Reshadat, S., Habtemariam, S., Iranshahy, M., Hasanpour, M., 2021. Perspective on the application of medicinal plants and natural products in wound healing: a mechanistic review. Pharmacol. Res. 174, 105841.